


Plastic Recycling Hot Paper
How to cite: *Angew. Chem. Int. Ed.* **2021**, *60*, 5527–5535

International Edition: doi.org/10.1002/anie.202011063

German Edition: doi.org/10.1002/ange.202011063

Towards the Circular Economy: Converting Aromatic Plastic Waste Back to Arenes over a Ru/Nb₂O₅ Catalyst

Yaxuan Jing, Yanqin Wang,* Shinya Furukawa, Jie Xia, Chengyang Sun, Max J. Hülsey, Haifeng Wang, Yong Guo, Xiaohui Liu, and Ning Yan*

Abstract: The upgrading of plastic waste is one of the grand challenges for the 21st century owing to its disruptive impact on the environment. Here, we show the first example of the upgrading of various aromatic plastic wastes with C–O and/or C–C linkages to arenes (75–85 % yield) via catalytic hydrolysis over a Ru/Nb₂O₅ catalyst. This catalyst not only allows the selective conversion of single-component aromatic plastic, and more importantly, enables the simultaneous conversion of a mixture of aromatic plastic to arenes. The excellent performance is attributed to unique features including: (1) the small sized Ru clusters on Nb₂O₅, which prevent the adsorption of aromatic ring and its hydrogenation; (2) the strong oxygen affinity of NbO_x species for C–O bond activation and Brønsted acid sites for C–C bond activation. This study offers a catalytic path to integrate aromatic plastic waste back into the supply chain of plastic production under the context of circular economy.

Introduction

At present, 380 million tons of plastics are produced around the world each year, and ≈80 % of which end up discarded.^[1] Due to the decades—or even centuries—long degradation kinetics, a majority of all plastics ever produced

on earth are still lying either in land or in oceans.^[1e,2] Many of the widely used plastics, such as polyethylene terephthalate (PET), polystyrene (PS), polycarbonate (PC), and polyphenylene oxide (PPO), are constructed from aromatic monomers by interunit C–O and/or C–C linkages.^[3] Indeed, PET, PS and PC are all listed among the top ten plastics used globally.^[4] These aromatic plastics are produced on an annual scale of ≈60 million tons, out of which ≈50 million tons are disposed into earth's ecosystem.^[3b] Commercialized route to reuse them mainly relies on mechanical recycling. Unfortunately, this method is associated with deteriorated properties of plastics which significantly limits its applicability.^[1a,3b,5] For example, only 7 % of recycled PET can be used to recast bottles.^[6]

So far, reports on chemical degradation of plastic waste were mainly focused on pyrolysis, which allows to handle relatively mixed plastic waste streams, especially polyolefins, PS and polymethyl methacrylate.^[3b,7] Alternative strategies (e.g., hydrolysis, alcoholysis, hydrogenation and aminolysis) have been developed to handle specific aromatic plastics in particular PET,^[3b,8] however, none of these are capable of converting a mixture of aromatic plastics necessitating sorting as a prerequisite. Considering the strong desire to minimize plastic disposal into the environment, and the increasing aspiration to generate profit by plastic reuse and recycling for the petro-chemical sector,^[3b,8f] developing advanced catalytic approaches for the upcycling of aromatic plastic waste into value-added chemicals is highly desirable.

Arenes (e.g., *p*-xylene, *m*-xylene, ethylbenzene, benzene)—predominantly derived from fossil fuels—are important raw materials for the manufacture of aromatic plastics and fibers. In order to achieve a circular economy, the conversion of aromatic plastic waste back to those arenes must be realized (Figure 1). In recent years, the production of arenes from non-petroleum based feedstock such as biomass and CO₂ gained particular attention, presenting an important field of research.^[9] Compared to biomass and CO₂, aromatic plastic waste has prominent advantages, including simpler molecular structure, much lower oxygen contents and abundant aromatic functionality (Figure S1). In particular, its simple structure, contrasting the complexity of biomass, provides grand opportunities to selectively produce a narrow stream of arenes, such as in the conversion of PET to *p*-xylene and PPO to *m*-xylene. To date, the selective degradation of aromatic plastic waste into target arenes is exceedingly rare. A key challenge of this task is to identify a catalyst that enables the selective cleavage of C–O and/or C–C bonds while preserving the aromatic rings. Inspired by C–O/C–C

[*] Y. Jing, Prof. Dr. Y. Wang, J. Xia, C. Sun, Prof. Dr. H. Wang, Dr. Y. Guo, Dr. X. Liu

Key Laboratory for Advanced Materials and Joint International Research Laboratory of Precision Chemistry and Molecular Engineering, Feringa Nobel Prize Scientist Joint Research Center, Research Institute of Industrial Catalysis, School of Chemistry and Molecular Engineering, East China University of Science and Technology

Shanghai 200237 (China)

E-mail: wangyanqin@ecust.edu.cn

Y. Jing, M. J. Hülsey, Prof. Dr. N. Yan

Department of Chemical & Biomolecular Engineering, National University of Singapore

4 Engineering Drive 4, Singapore 117585 (Singapore)

E-mail: ning.yan@nus.edu.sg

Prof. Dr. S. Furukawa

Institute for Catalysis, Hokkaido University

N-21, W-10, Sapporo 001-0021 (Japan)

and

Elements Strategy Initiative for Catalysis and Battery, Kyoto University

Kyoto Daigaku Katsura, Nishikyo-ku, Kyoto 615-8510 (Japan)

 Supporting information and the ORCID identification number(s) for the author(s) of this article can be found under:

 <https://doi.org/10.1002/anie.202011063>.

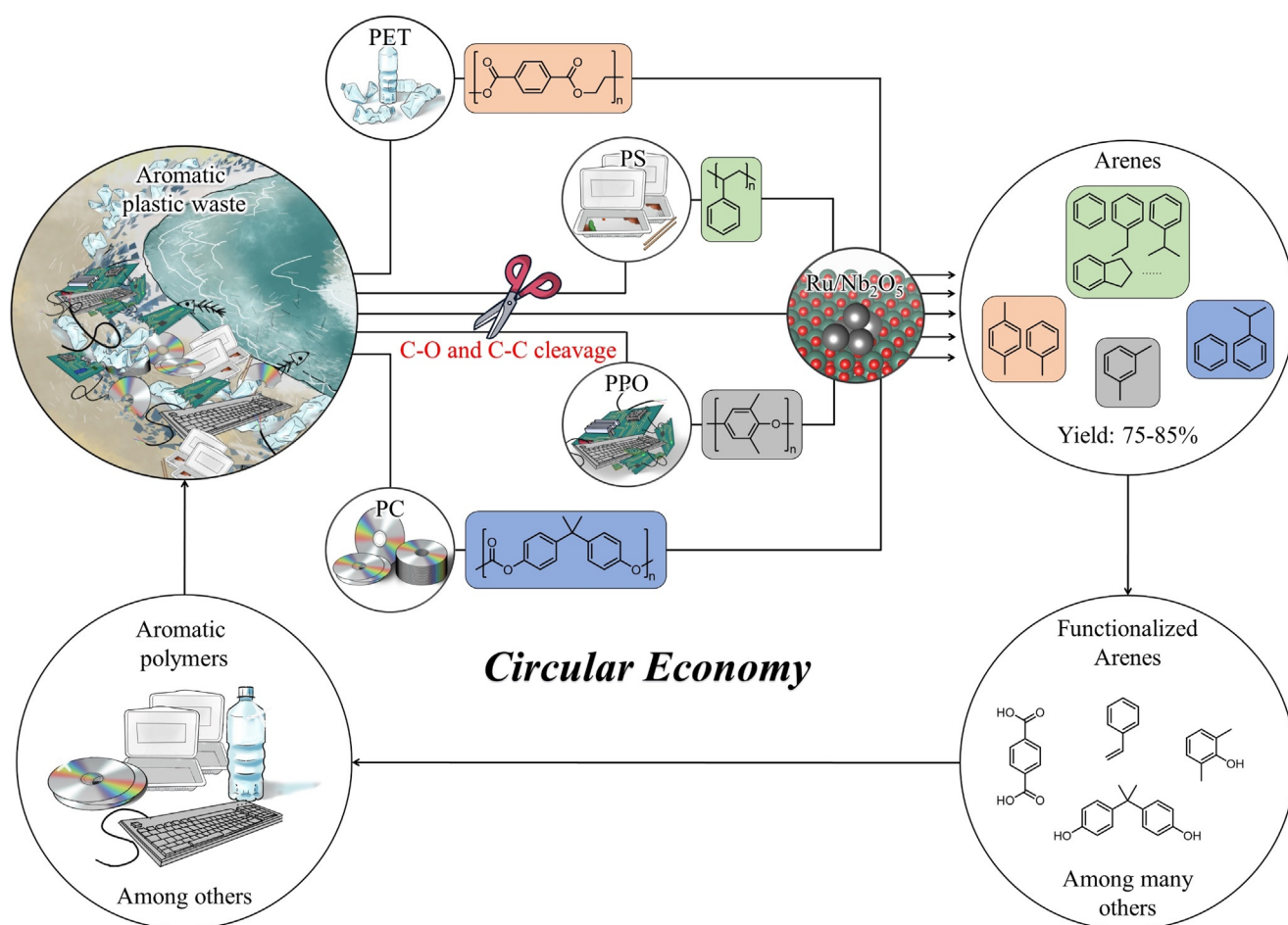


Figure 1. The integration of a C–O and C–C bond cleavage catalyst into the circular plastic economy. Ru/Nb₂O₅ is proposed as a possible catalyst for the conversion of various aromatic plastic waste (PET = polyethylene terephthalate, PS = polystyrene, PPO = poly(*p*-phenylene oxide), PC = polycarbonate) and mixtures thereof into arenes.

activation chemistry, cooperative catalysis between two or more different active sites, especially a combination of metal sites with high hydrogenation property and acidic supports with the strong ability to activate C–O/C–C bonds, is required to overcome this key challenge. Up to now, no catalyst can realize this ambitious goal.

Herein, we report that a multifunctional Ru/Nb₂O₅ catalyst can directly upgrade aromatic plastic waste into arenes in unusually high yields (Figure 1). We demonstrate that Ru/Nb₂O₅ does not only catalyze the selective conversion of single-component plastic waste into bulk chemicals (PET to *p*-xylene and PPO to *m*-xylene), but also enables the conversion of mixed aromatic plastics into arenes. This catalyst combines two key functions, namely NbO_x species for C–O bond activation and Brønsted acid sites for C–C bond activation, respectively, making the production of monocyclic arenes feasible. We confirmed that Ru species on Nb₂O₅ present as sub-nano particles with low coordination number (C.N. = 5–6), preventing the hydrogenation of the benzene ring thus affording a distinct selectivity to arenes. To the best of our knowledge, this is the first time to achieve the upgrading of aromatic plastic waste into arenes through the

selective cleavage of interunit C–O and/or C–C linkages, and the catalytic performance of Ru/Nb₂O₅ is unparalleled by other catalysts.

Results and Discussion

PET, PPO, PS and PC are chosen as model compounds since they comprise all common types of linkages in aromatic plastics, namely ester linkage, ether linkage, C–C and combinations of C–O and C–C linkages. Moreover, PET, PS and PC represent the largest three groups produced among various aromatic plastics.^[16,4] Initially, PET, PPO, PS and PC from commercial sources were analyzed by FT-IR and elemental analysis (Figure S2 and Table S1). The results confirmed the chemical structure and relatively high purity of these plastics,^[10] offering the basis to calculate product yields in catalytic reactions. The shape and porous properties of Nb₂O₅ and Ru/Nb₂O₅ are provided in Figure S3.

The conversion of PET into *p*-xylene in aqueous solution was employed as a probe reaction to investigate the cleavage of interunit C–O linkages (Figure 2a). The main reason we

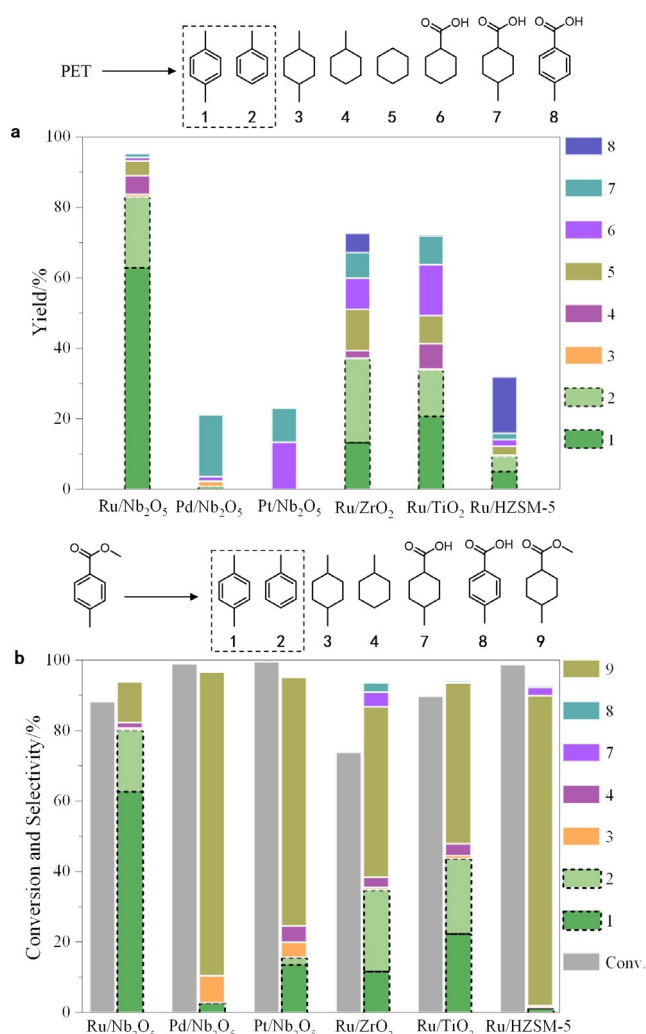


Figure 2. The conversion of PET over various catalysts. a, The direct conversion of PET over various catalysts. Reaction conditions: 0.1 g PET, 0.1 g catalyst, 10 g H₂O, 200 °C, 12 h, 0.3 MPa H₂; b, The conversion of methyl *p*-toluate over various catalysts. Reaction conditions: 0.05 g methyl *p*-toluate, 0.025 g catalyst, 5 g H₂O, 200 °C, 3 h, 0.3 MPa H₂.

use water as solvent is that water is a polar solvent that binds reasonably strongly with polar functionalities in PET. This helps to weak the inter-chain interactions. Moreover, water does not react with hydrogen over metal-solid acid catalysts at the reaction temperature. In contrast, some common polar organic solvents, such as THF, acetone, ethanol et al, may suffer from hydrogenation/hydrogenolysis reactions.^[11] Among all catalysts (Ru/Nb₂O₅, Pd/Nb₂O₅, Pt/Nb₂O₅, Ru/TiO₂, Ru/ZrO₂ and Ru/HZSM-5) investigated, Ru/Nb₂O₅ gave an exceptional yield of monomers (95.2%) and a high selectivity to arenes (87.1%) (calculated based on the ratio between the mole of product and the mole of aromatic units in polymer feedstock). Over Pd/Nb₂O₅ and Pt/Nb₂O₅, a total monomer yield of ≈ 20% was obtained, much lower than that over Ru/Nb₂O₅. Noteworthy, the main products obtained in the latter two cases were ring saturated products (compound 6 & 7 in Figure 2). Hence, we suspected the poor performance of Pd and Pt catalysts was due to the fast hydrogenation of

aromatic rings, resulting in the formation of chemically more robust C–O linkages. To verify this, we conducted the conversion of methyl *p*-toluate over Nb₂O₅-loaded Ru, Pt, and Pd catalysts (Figure 2b) and observed arenes as the main products over Ru/Nb₂O₅ (80.1% selectivity). In sharp contrast, the main product was ring-saturated compound 9 over Pt/Nb₂O₅ and Pd/Nb₂O₅. This result indicates that Pd- and Pt-based catalysts are more active for the hydrogenation of benzene rings, and that the cleavage of C–O bonds in the saturated ring is more challenging. The latter was further confirmed by employing compound 9 as substrate (Table S2), whose conversion is only 13.6% under the same conditions. Two factors are involved in the poor reactivity. First, the C–O bond energy in compound 9 is higher than that in methyl *p*-toluate because of the conjugation effect between the benzene ring and the ester group. In addition, the conjugated aromatic group has a planar structure, resulting in a smaller steric hindrance compared to non-planar cyclohexane rings. Therefore, the activation of C–O bonds adjacent to saturated rings is not favorable, which highlights the significance of preserving aromatic rings. In the case of Nb₂O₅-supported catalysts, Ru with appropriate hydrogenation ability, instead of Pd and Pt, is the most selective metal site.

With Ru/ZrO₂, Ru/TiO₂ and Ru/HZSM-5 as catalysts, total monomer yields of 72.6, 71.9 and 31.8%, respectively, were obtained from PET, lower than that over Ru/Nb₂O₅ (95.2%). Interestingly, the selectivity of arenes also decreased dramatically (50.8, 46.7 and 28.9%). Those results imply that Ru species on these three supports, unlike Ru species on Nb₂O₅, tend to hydrogenate the aromatic ring. The conversion of methyl *p*-toluate was conducted over these four catalysts (Figure 2b). Indeed, the unusual selectivity towards arenes was only achieved over Ru/Nb₂O₅, while it was lower than 50% with compound 9 as the main product over the other three catalysts.

Previously we found that NbO_x species in Nb-based catalysts have the unique ability to activate C–O bonds in biomass.^[11] It is therefore not unreasonable to speculate that besides the uncommon properties of Ru clusters on Nb₂O₅ to preserve benzene rings, Nb₂O₅ itself plays an important role in C–O bond cleavage. To confirm this, we employed compound 9 as substrate to compare Ru-based catalysts under relatively harsh conditions (220 °C, 4 h, 3 MPa H₂) (Figure S5). As expected, the highest conversion and selectivity to 1,4-dimethylcyclohexane were achieved over Ru/Nb₂O₅, in agreement with previous results on the hydrodeoxygenation of biomass and its derivatives,^[11] thus confirming NbO_x species possess a strong ability to activate the C–O bonds in plastics. Combining all experimental observations, we attribute the exceptional performance of Ru/Nb₂O₅ to an effective synergism of the support-mediated C–O bond activation and the metal-based selective hydrogenation. The influence of reaction conditions was investigated. The major findings include: (1) the plastic conversion increased monotonically as a function of time while there was little variations of selectivity towards each product; (2) lower temperature led to low reaction rates, whereas higher temperature favored the undesirable decarboxylation; (3) higher pressure favored the hydrogenation of aromatic ring, whereas lower pressure was

not able to complete deoxygenation. Detailed discussions are provided in the Supporting Information (Figure S6). Finally, the direct conversion of Coca-Cola bottle was tested over Ru/Nb₂O₅ and encouragingly, a total monomer yield of 90.9% was achieved with an arene selectivity of 78.4% (table S3), confirming the applicability of the established system to upgrade real PET waste.

We next tested the conversion of PPO, an ether-linked plastic, over Ru/Nb₂O₅ with water and octane as medium. PPO aggregated into a solid globule after the reaction in water, whereas desirable *m*-xylene was successfully obtained in octane. The dissolution/swelling of PPO in two solvents was compared through stirring at room temperature and it was observed that PPO dispersed better in octane than in water (Figure S7). Therefore, octane was employed as reaction medium to perform the conversion of various aromatic plastics. PET was effectively converted to arenes (83.6% yield) in octane (Figure 3) as well. A high yield (85.0%) of *m*-xylene was achieved starting from PPO, demonstrating that, besides the ability to convert ester-linked plastics, Ru/Nb₂O₅ also enabled the degradation of ether-linked plastics.

Our objective is to cleave all types of interunit C–O/C–C linkages in aromatic plastic waste to produce arenes. Hence, we conducted the conversion of PS formed solely via C–C linkages over Ru/Nb₂O₅. Notably, the conversion of PS afforded a total monocyclic arenes yield of 75.9%. It should be noted that the cleavage always occurs at the sp²-sp³ bond, namely the C_{aromatic}–C connected with aromatic rings, thus affording high selectivity to benzene, which is highly consistent with our previous report in lignin conversion.^[12] A certain amount of indane derivatives and other arenes were generated by the acid-catalyzed alkylation. This result proved that Ru/Nb₂O₅ is effective in breaking the C–C linkages in aromatic plastic waste while preserving aromatic rings. Previously, degradation of plastics formed via stable C–C linkages predominately rely on the non-selective pyrolysis

route to pyrolysis oil and then may be further upgraded into arenes via zeolite-catalyzed aromatization.^[3b] Our newly established system is distinct from conventional pyrolysis process that enables the selective cleavage of the C_{aromatic}–C linkages to directly produce monocyclic arenes.

To evaluate the catalyst performance with increasing feedstock complexity, PC comprising both ester and C–C linkages was chosen. The corresponding monocyclic aromatic hydrocarbons were obtained in 83.3% total yield, indicating the simultaneous, efficient cleavage of both bond types already hinting at the possibility to convert mixtures of aromatic plastic waste. It is noteworthy that the PC used here is commercial polycarbonate board, once again confirming that the catalytic system is able to work well to address real PC waste. We further evaluated the potential of Ru/Nb₂O₅ for the direct conversion of mixed plastics containing PET, PS, PC and PPO. Encouragingly, the mixture underwent the cleavage of interunit C–O and C–C bonds to yield the arenes expected from single component conversion experiments with a total yield of 78.9%, confirming the applicability of Ru/Nb₂O₅ to convert mixtures of plastic waste without interference of individual plastic component. The concentration of substrate was investigated (Figure S8) and the results show a negligible decrease in arenes yield (from 78.9% to 75.3%) occurs when the concentration was increased from 1.5% to 3%, strengthening the potential of this new system. The mass ratio of substrate to catalyst was increased from 1/1 to 2/1, the arenes yield reduced slightly (from 78.9% to 68.8%), indicating that unlike biomass conversion,^[9] the contact problem between plastic and catalyst has a relatively little influence on the reaction since plastics can melt under high temperature (generally > 250°C) and Ru/Nb₂O₅ is capable of producing a high throughput in such circumstances.

Catalyst recycling was conducted with mixed plastics as feedstock and some activity lost (≈ 28%) in the second run (Figure S9a). From TG analysis (≈ 10% carbon deposition on spent catalyst, Figure S9b), we speculate that the activity loss may come from the coverage of active sites by carbon. Indeed, after calcination in air (450°C for 3 h) followed by reduction using H₂ (400°C for 2 h), the catalyst was recharged for the next run and the same arene yield was obtained, even after 3 cycles. The consistent high yields of arenes, and the absence of any change in XRD patterns for the spent catalyst (Figure S9c), clearly demonstrate the high durability of Ru/Nb₂O₅ catalyst.

An intriguing question is why Ru/Nb₂O₅ can not only catalyze the C–O and C–C bond cleavage efficiently, but also gives distinct selectivity to arenes. Detailed characterizations were conducted to understand the structure of the catalyst and its structure–activity correlations. Although no diffraction peaks corresponding to Ru (Figure S10) were identified in the XRD patterns of all Ru-based samples, the Ru dispersion results revealed that Ru on Nb₂O₅ is substantially higher dispersed (73.4%) than on other supports such as Ru/ZrO₂ (21.1%), Ru/TiO₂ (7.7%), and Ru/HZSM-5 (15.8%), suggesting the presence of smaller Ru species on Nb₂O₅ (Table S6). The H₂-TPR profiles (Figure 4a) indicated that the reduction temperature of Ru on Ru/Nb₂O₅ (130°C) was higher than that of Ru/ZrO₂ (106°C), Ru/TiO₂ (105°C) and

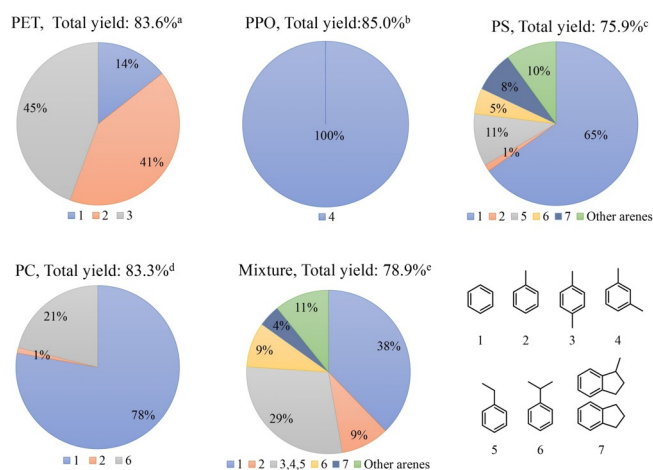


Figure 3. Results of the conversion of various aromatic plastics over Ru/Nb₂O₅. Reaction conditions: 30 mg feedstock, 30 mg Ru/Nb₂O₅, 4 g octane, 0.5 MPa H₂. a) 280°C, 8 h; b) 280°C, 16 h; c) 300°C, 16 h; d) 320°C, 16 h; e) Reaction conditions: 15 mg PET, 15 mg PC, 15 mg PS, 15 mg PPO, 60 mg Ru/Nb₂O₅, 4 g octane, 0.5 MPa H₂, 320°C, 16 h.

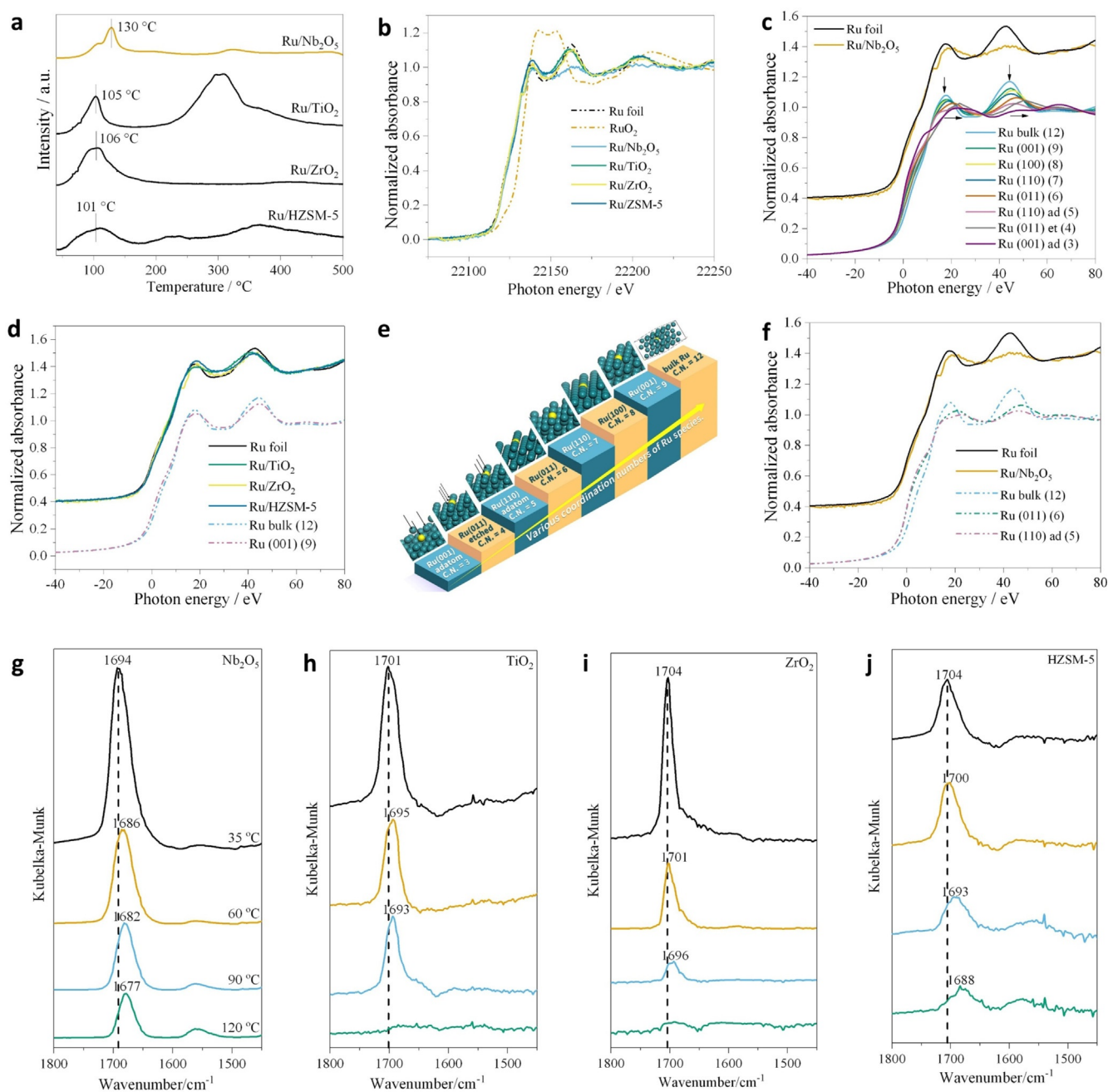


Figure 4. Characterization of oxide-supported Ru catalysts. a, H_2 -TPR profiles of various catalysts; b, XANES spectra of various Ru-based catalysts; c, XANES simulation by DFT with a series of Ru coordination numbers; d, comparison of XANES spectrum of other Ru catalysts and DFT-calculated spectra; e, Various coordination numbers of Ru species considered for XANES simulation; f, comparison of XANES spectra of Ru/Nb $_2$ O $_5$ and DFT-calculated spectra; acetone DRIFTS spectra for g, Nb $_2$ O $_5$, h, TiO $_2$, i, ZrO $_2$, and j, HZSM-5, at increasing temperatures of 35 °C (black), 60 °C (orange), 90 °C (blue), and 120 °C (green).

Ru/HZSM-5 (101 °C), implying the strong interaction between Ru and Nb $_2$ O $_5$.

X-ray absorption near-edge structure (XANES) analysis was carried out to further clarify the chemical state and coordination environment of Ru (Figure 4b). Ru species on all catalysts are close to metallic zero-valent state. XANES spectra of Ru on ZrO $_2$, TiO $_2$ and HZSM-5 are identical to that of Ru foil, suggesting that Ru species with high Ru-Ru coordination numbers are dominant on these supports. In sharp contrast, the XANES spectrum of Ru on Nb $_2$ O $_5$ has

evidently different amplitude of the fine structure oscillations, although the Ru is also zero-valent. This smaller amplitude indicates that Ru on Nb $_2$ O $_5$, unlike Ru species on other supports and Ru foil, has a different coordination environment. We conducted the Ru K-edge extended X-ray absorption fine structure (EXAFS) analysis, and the fitting results for Ru/TiO $_2$ and Ru/ZSM-5 (Figure S11) demonstrate coordination numbers at around 9 for Ru in Ru/TiO $_2$ and Ru/ZSM-5 catalysts (Table S7). On the other hand, the extended scattering paths (measured by transmission or fluorescence

mode) for Ru/Nb₂O₅ and Ru/ZrO₂ could not be analyzed due to the large X-ray absorption by Nb and Zr and the overlap of major Ru K_{α1} emission with K_{β2} of Nb and Zr, respectively. Based on the fact that Nb₂O₅-supported Ru has a higher dispersion, we suspect that Ru on Nb₂O₅ may tend to be low-coordinated with small particle sizes.

XANES spectra are commonly used to reveal the chemical states of metals, however, less attention has been paid to explore the information of how coordination environment and particle size affect XANES spectra.^[13] Here, we successfully estimated the geometric configuration of Ru species on the Nb₂O₅ support by comparing the experimental and density functional theory (DFT) predicted Ru XANES spectra. All shapes including corner, edge, face and bulk atoms with various coordination numbers (C.N. = 3–9, 12) of Ru species considered for XANES simulation are presented in Figure 4e. Arc tangent functions were generated to calibrate the baseline so that the simulation well reproduces the experimental spectrum of the Ru foil (Figure S12). The XANES simulations by DFT calculations (Figure 4c) allows a full assignment of the spectra for a series of Ru coordination numbers (C.N. = 3–9, 12). The calculated spectra show that the peak intensity decreases while the peak position shifts to higher energy with the decrease of coordination numbers. This is probably because the electron density on the coordinatively unsaturated Ru becomes higher due to the larger number of dangling bonds. Not unexpectedly, comparison between experimental and theoretical spectra (Figure 4d) shows that XANES spectra of Ru species on ZrO₂, TiO₂ and HZSM-5 are very similar to those of Ru with C.N. = 9 or 12, confirming the EXAFS fitting results. Remarkably, the XANES spectrum of Ru/Nb₂O₅ resembles those simulated for Ru with C.N. = 5 or 6 very closely, providing strong evidence that the major Ru species on Nb₂O₅ are those with low coordination numbers (C.N. = 5–6) (Figure 4f). Such low coordination numbers indicate that the contribution of edge sites is dominant, confirming that the dimension of Ru on the Nb₂O₅ support is in the sub-nanometer range.

It is known that the effective co-adsorption of aromatic rings and H₂ is a prerequisite to catalyze the hydrogenation of the aromatic ring. It is therefore reasonable to believe that the limited surface area of small Ru clusters on Nb₂O₅ restrain the co-adsorption of H₂ and aromatic rings due to the increased barrier for aromatic ring adsorption on metal clusters compared to flat surfaces,^[14] resulting in a unique selectivity to arenes. Meanwhile, the adsorption of H₂ is less affected by the particle size effect and therefore Ru sub-nano particles maintain sufficient capability of H₂ dissociation to assist C–O/C–C cleavage.

The oxygen affinity and C–O bond activation capability of the support are essential factors for the conversion of bonds prevalent in plastics.^[9a,11b] To verify the oxygen affinity of Nb₂O₅, acetone as a simple oxygen-containing molecule, was selected to perform adsorption-desorption DRIFTS experiments on various supports (Figure 4g–j). For acetone, the peak at 1740 cm⁻¹ is assigned to the C=O stretching vibration.^[15] The red shift on Nb₂O₅ (1694 cm⁻¹) is evidently stronger than that on ZrO₂ (1704 cm⁻¹), TiO₂ (1701 cm⁻¹), and HZSM-5 (1704 cm⁻¹) after purging with N₂ for 30 min at

35°C, indicating that Nb₂O₅ possesses stronger activation ability than other supports. When the purging temperature rose to 120°C, acetone on ZrO₂ and TiO₂ desorbed completely while minimum C=O bond signal on HZSM-5 was observed. On Nb₂O₅, in contrast, the peak of C=O bond was still clearly visible, providing evidence that Nb₂O₅ has distinctively strong adsorption capability to oxygen-containing groups. With the help of dissociated H species over Ru clusters, the unique synergistic activity for the cleavage of C–O bonds within aromatic plastics is rationalized.

The performance of Ru/Nb₂O₅ and Ru/HZSM-5 on C–C bond cleavage was tested using diphenylmethane as a model compound (Table S8). Over Ru/Nb₂O₅, the desirable C–C cleavage products (benzene and toluene) were generated. Over Ru/HZSM-5, ring-saturated products are predominant, indicating that the hydrogenation of benzene ring is favored compared with the desired C–C bond cleavage. The very low total product yield (4.5%) at a conversion of 17.6% was caused by the cracking of substrate and products over Ru/HZSM-5. Therefore, Ru/Nb₂O₅ has superior performance for the desirable C–C bond cleavage over Ru/HZSM-5.

We conducted the blank experiments and selected PET and PS as starting materials because PET and PS representing C–O and C–C linked plastic, respectively. The results are present in Table S4. For PET conversion, terephthalic acid as the only product was found in catalyst-free and Nb₂O₅ conditions, indicating that conventional hydrolysis of PET can occur over Nb₂O₅ or in pure water under high reaction temperature. As to the conversion of PS over Nb₂O₅ and catalyst-free conditions, no products were detected. Furthermore, no conversion was observed under catalyst-free or pure Nb₂O₅ condition when diphenylmethane was employed as a model compound to test the C–C cleavage performances. These results show that the C–C cleavage of PS only occurs over the multifunctional Ru/Nb₂O₅ catalyst.

We conducted DRIFTS analysis of toluene adsorption to compare the adsorption-activation of benzene ring on Nb₂O₅ and HZSM-5 (Figure 5). The peaks at 3450 and 1623 cm⁻¹ are attributed to hydrogen-bonded OH stretching and HOH bending vibration of the adsorbed water molecules (Figure S14). For gas phase toluene, the peaks at 1454–1603 cm⁻¹ and 3026–3085 cm⁻¹ are ascribed to the stretching mode of the C=C bonds and C–H stretching mode of benzene ring, respectively. The same spectra for Ru/Nb₂O₅ and Nb₂O₅ (Figure S15) confirm that the primary adsorption sites reside on Nb₂O₅ and Ru has little effect on adsorption of benzene ring. While with the purging temperature rising from 30 to 90°C, two clear red-shifts at 1603 cm⁻¹ (Δ = 6 cm⁻¹) and 1454 cm⁻¹ (Δ = 5 cm⁻¹) were observed over Nb₂O₅, suggesting that C=C vibrations are hindered because of the adsorption-activation of benzene ring on Nb₂O₅ (Figure 5a). Meanwhile, an obvious blue-shift (Δ = 6 cm⁻¹) at 3058 cm⁻¹ was found on Nb₂O₅ probably because the C–H vibrations became stronger (Figure 5b). The blue-shift provides additional evidence for the adsorption-activation of benzene ring on Nb₂O₅, where the strong adsorption-activation to benzene ring framework lengthens the C–H bonds, resulting in the stronger C–H vibrations. In marked contrast to Nb₂O₅, no corresponding red- or blue-shift was observed on HZSM-5 when the purging

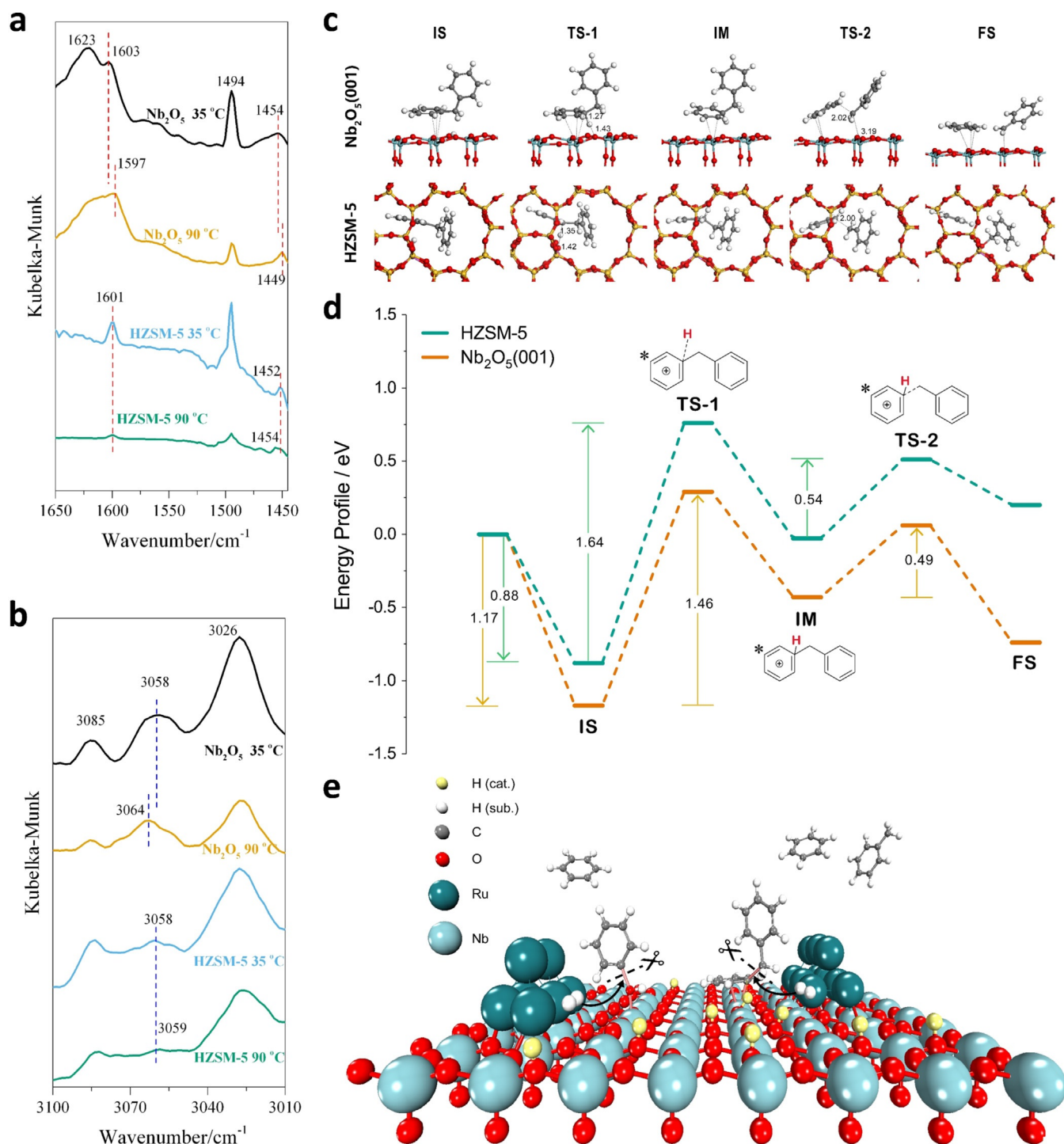


Figure 5. a, Toluene DRIFTS spectra (1454–1603 cm⁻¹) of Nb₂O₅ and HZSM-5; b, Toluene DRIFTS spectra (3026–3085 cm⁻¹) of Nb₂O₅ and HZSM-5; c, Optimized structures of diphenylmethane adsorption on Nb₂O₅ and HZSM-5, diphenylmethane adsorption (IS); TS of protonation (TS-1), intermediate state (IM), TS of Csp²-Csp³ cleavage (TS-2) and final state (FS); d, Energy profiles of the Csp²-Csp³ cleavage processes of diphenylmethane; e, Proposed mechanism of catalytic C-O/C-C cleavage over Ru/Nb₂O₅.

temperature rise to 90 °C, providing evidence that Nb₂O₅ has distinctively stronger adsorption-activation capability to benzene than that of HZSM-5.

Next, DFT calculations were performed to comparatively investigate the C_{sp²-C_{sp³ cleavage of diphenylmethane over Nb₂O₅(001) and HZSM-5. The optimization of adsorption}}

sites confirms that on Nb₂O₅, the primary adsorption sites of benzene ring reside on NbO_x species, but on HZSM-5, Brønsted acid sites as adsorption sites have the priority over AlO_x species (Figure S15). Optimized structures of this process and the reaction energy profile are shown in Figure 5c and 5d. Firstly, the adsorption energy of diphenyl-

methane on Nb₂O₅(001) (−1.17 eV) is larger than that on HZSM-5 (−0.88 eV), in good agreement with the DRIFTS results, where Nb₂O₅ enables stronger adsorption to benzene ring. It is noteworthy that the carbocation intermediate formed by the Brønsted acid sites-driven protonation process is crucial for the C_{sp2}–C_{sp3} cleavage, given that the direct C_{aromatic}–C bond cleavage is extremely difficult.^[12] Furthermore, we quantitatively calculated the reaction energies and energy barriers of protonation process and C_{sp2}–C_{sp3} cleavage of the protonated intermediate (C₆H₅(H)C₇H₇⁺), respectively. The following key information are obtained: (i) On Nb₂O₅, both steps show evidently lower kinetic barriers than these on HZSM-5; (ii) the whole reaction energy change of the C–C cleavage on Nb₂O₅ (0.43 eV) is lower than that on the HZSM-5 (1.09 eV). From above, Nb₂O₅ is superior to HZSM-5, since it facilitates the protonation, C_{sp2}–C_{sp3} cleavage and modified the overall reaction energy profile.

The above study confirmed that the multifunctional Ru/Nb₂O₅ catalyst plays two roles in the selective cleavage of C–O/C–C bonds in aromatic plastic waste into arenes: 1) small size Ru species with low coordination numbers (C.N. = 5–6) as hydrogenation sites limit co-adsorption of H₂ and aromatic rings, affording a high selectivity to arenes; 2) NbO_x is responsible for the activation of C–O bonds and benzene ring while Brønsted acid sites assist in cleaving C–C bonds. The cooperative effect between small-sized Ru, NbO_x species and Brønsted acid sites render this catalyst exceptionally suitable for the decomposition of plastic mixtures into arenes. The cooperative effects of different components of catalyst are highlighted in Figure 5 e. For C–O bond cleavage, Lewis acid sites (NbO_x species) enable the selective adsorption and activation of C–O bond. Then, with the help of dissociated H species over Ru, the cleavage of C–O bonds in aromatic plastics is efficiently achieved. For C–C bond cleavage, benzene ring is first adsorbed on Lewis acid sites (NbO_x species) of Nb₂O₅, then the adsorbed benzene ring is protonated by Brønsted acid sites on Nb₂O₅ to proceed the activation of the C_{sp2}–C_{sp3} bond. Following that, the dissociated H species on Ru clusters attack the weakened C_{sp2}–C_{sp3} bond to break it. The small Ru clusters play a key role to achieve highly selective arene production during C–O/C–C cleavage, where the limited surface of small Ru clusters restrain the co-adsorption of H₂ and aromatic rings.

Based on experimental data, we performed a preliminary mass balance analysis for the new route (Figure 6). Starting

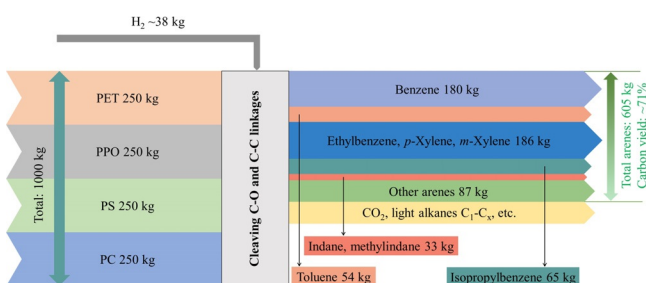


Figure 6. Mass balance of aromatic plastics into arenes. The values are estimated based on the reaction stoichiometries in this study and assuming the conversion of 1 ton feedstocks.

from 1 ton aromatic plastic mixture, 60.5 wt% of the feedstock can be converted into arenes in a single-step with the consumption of only 3.8 wt% H₂, which compares favorably with other emerging technologies for renewable arene production from woody biomass and CO₂ (Figure S16 and S17). Only 20.7–34.4 wt% of 1 ton raw woody biomass and 9.8–15.8 wt% of 1 ton CO₂- significantly lower than for aromatic plastics valorization-can be converted into arenes based on open data in the literature (Figure S16a and S17a). Moreover, the additional use of ethylene for biomass conversion and the much higher demand of H₂ for CO₂ hydrogenation inevitably increase the cost of the competing technologies. As a result, the newly established route adds a promising option with unequaled efficiency for arene production from waste resources. The separation of arenes can be achieved through distillation. For isomers, such as *p*-xylene and *m*-xylene, adsorption is a viable approach.^[21]

Conclusion

In summary, we have developed the direct upgrading of aromatic plastic waste mixtures back to arenes in high yield via the precise cleavage of interunit C–O and C–C linkages over a Ru/Nb₂O₅ catalyst. Ru/Nb₂O₅ is able to selectively break all common types of linkages in aromatic plastics, including ester, ether and even C–C linkages to obtain monocyclic arenes. Ru species on Nb₂O₅, unlike those on other supports, have ultra-small particle sizes, preventing the hydrogenation of aromatic rings. Along with NbO_x species for C–O bond activation and Brønsted acid sites for C–C bond cleavage, desired reactivity towards aromatic plastic depolymerization is achieved.

Despite the long-standing research efforts for chemical upgrading of plastic waste, a majority of previously developed routes is only applicable for specific plastic waste streams. Pyrolysis is an exception, since it enables the transformation of relatively mixed plastic waste streams, but still is unable to work well with the plastic contaminations including PVC, PU and PET.^[3b] Thus, a combination of different technologies may be applied in the future to provide a satisfactory solution of plastic waste valorization. The here reported catalytic system converting aromatic plastic waste into value-added arenes adds new options in plastic upcycling offering possible solutions to two key challenges, namely, the accumulation of highly persistent aromatic plastics in the environment and the excessive dependence on fossil fuels for the production of aromatic chemicals and downstream polymers.

We highlight the following limitations of the new approach deserving consideration and further development: a) Despite the superior catalytic performance of Ru/Nb₂O₅ in cleaving C–C and C–O bonds in plastics, the solid-solid contact problem between recalcitrant plastic and solid catalyst, remains a challenge. Designing advanced solvent system to increase plastic swelling and solubility is highly desirable; b) H₂ gas is used as a reductant. Establish hydrogen transfer systems using renewable alcohols and acids as hydrogen sources, is a way to reduce process complexity and cost; c) Non-noble-metal based catalysts with compara-

ble performance should be explored to improve the overall economic competitiveness. Developments along these lines are going on in our labs.

Acknowledgements

This work was supported financially by the NSFC of China (No. 21832002, 21872050, 21808063), the Science and Technology Commission of Shanghai Municipality (2018SHZDZX03), the Programme of Introducing Talents of Discipline to Universities (B16017) in China, the Fundamental Research Funds for the Central Universities (222201718003), and the NUS Flagship Green Energy Programme (R-279-000-553-646, and R-279-000-553-731). The XAS analysis was performed with the approval of Japan Synchrotron Radiation Research Institute (JASRI: No. 2019B1620). Computation time was provided by the super-computer systems in Institute for Chemical Research Kyoto University. Y. J. is grateful for financial support from the China Scholarship Council (CSC grant number 201906740056).

Conflict of interest

The authors declare no conflict of interest.

Keywords: arenes · circular economy · C–O/C–C cleavage · plastic · Ru/Nb₂O₅

- [1] a) *Nat. Catal.* **2019**, *2*, 945–946; b) V. Tournier, C. Topham, A. Gilles, B. David, C. Folgoas, E. Moya-Leclair, E. Kamionka, M.-L. Desrousseaux, H. Texier, S. Gavalda, *Nature* **2020**, *580*, 216–219; c) J. M. García, M. L. Robertson, *Science* **2017**, *358*, 870–872; d) J. R. Jambeck, R. Geyer, C. Wilcox, T. R. Siegler, M. Perryman, A. Andrady, R. Narayan, K. L. Law, *Science* **2015**, *347*, 768–771; e) R. Geyer, J. R. Jambeck, K. L. Law, *Sci. Adv.* **2017**, *3*, e1700782; f) B. F. S. Nunes, M. C. Oliveira, A. C. Fernandes, *Green Chem.* **2020**, *22*, 2419–2425; g) T. Uekert, M. F. Kuehnel, D. W. Wakerley, E. Reisner, *Energy Environ. Sci.* **2018**, *11*, 2853–2857; h) A. Rahimi, J. M. García, *Nat. Rev. Chem.* **2017**, *1*, 0046.
- [2] H. P. Austin, M. D. Allen, B. S. Donohoe, N. A. Rorrer, F. L. Kearns, R. L. Silveira, B. C. Pollard, G. Dominick, R. Duman, K. El Omari, *Proc. Natl. Acad. Sci. USA* **2018**, *115*, E4350–E4357.
- [3] a) C. J. Rhodes, *Sci. Prog.* **2018**, *101*, 207–260; b) I. Vollmer, M. J. Jenks, M. C. Roelands, R. J. White, T. van Harmelen, P. de Wild, G. P. van der Laan, F. Meirer, J. T. Keurentjes, B. M. Weckhuysen, *Angew. Chem. Int. Ed.* **2020**, *59*, 15402–15423; *Angew. Chem.* **2020**, *132*, 15524–15548.
- [4] a) World Plastics Production 1950–2015 (Plastics Europe); b) Plastics-the Facts 2019: An analysis of European plastics production, demand and waste data (Plastics Europe).
- [5] N. A. Rorrer, S. Nicholson, A. Carpenter, M. J. Bidy, N. J. Grundl, G. T. Beckham, *Joule* **2019**, *3*, 1006–1027.
- [6] T. Uekert, H. Kasap, E. Reisner, *J. Am. Chem. Soc.* **2019**, *141*, 15201–15210.
- [7] a) A. B. Raheem, Z. Z. Noor, A. Hassan, M. K. A. Hamid, S. A. Samsudin, A. H. Sabeen, *J. Clean. Prod.* **2019**, *225*, 1052–1064; b) R. Aguado, M. n. Olazar, B. Gaisán, R. Prieto, J. Bilbao, *Chem. Eng. J.* **2003**, *92*, 91–99; c) M. Artetxe, G. Lopez, M. Amutio, G. Elordi, M. Olazar, J. Bilbao, *Ind. Eng. Chem. Res.* **2010**, *49*, 2064–2069.
- [8] a) S. Westhues, J. Idel, J. Klankermayer, *Sci. Adv.* **2018**, *4*, eaat9669; b) H. Tang, N. Li, G. Li, A. Wang, Y. Cong, G. Xu, X. Wang, T. Zhang, *Green Chem.* **2019**, *21*, 2709–2719; c) H. Tang, Y. Hu, G. Li, A. Wang, G. Xu, C. Yu, X. Wang, T. Zhang, N. Li, *Green Chem.* **2019**, *21*, 3789–3795; d) E. Feghali, T. Cantat, *ChemSusChem* **2015**, *8*, 980–984; e) X. Jiao, K. Zheng, Q. Chen, X. Li, Y. Li, W. Shao, J. Xu, J. Zhu, Y. Pan, Y. Sun, Y. Xie, *Angew. Chem. Int. Ed.* **2020**, *59*, 15497–15501; *Angew. Chem.* **2020**, *132*, 15627–15631; f) X. Zhang, M. Fevre, G. O. Jones, R. M. Waymouth, *Chem. Rev.* **2018**, *118*, 839–885.
- [9] a) Y. Jing, Y. Guo, Q. Xia, X. Liu, Y. Wang, *Chem* **2019**, *5*, 2520–2546; b) W. Schutyser, T. Renders, S. Van den Bosch, S. F. Koelewijn, G. T. Beckham, B. F. Sels, *Chem. Soc. Rev.* **2018**, *47*, 852–908; c) X. Wu, X. Fan, S. Xie, J. Lin, J. Cheng, Q. Zhang, L. Chen, Y. Wang, *Nat. Catal.* **2018**, *1*, 772–780; d) Z. R. Zhang, J. L. Song, B. X. Han, *Chem. Rev.* **2017**, *117*, 6834–6880; e) W. Zhou, K. Cheng, J. Kang, C. Zhou, V. Subramanian, Q. Zhang, Y. Wang, *Chem. Soc. Rev.* **2019**, *48*, 3193–3228; f) S. Saeidi, N. A. S. Amin, M. R. Rahimpour, *J. CO₂ Util.* **2014**, *5*, 66–81; g) A. E. Settle, L. Berstis, N. A. Rorrer, Y. Roman-Leshkóv, G. T. Beckham, R. M. Richards, D. R. Vardon, *Green Chem.* **2017**, *19*, 3468–3492.
- [10] a) M. Liang, Y.-J. Jhuang, C.-F. Zhang, W.-J. Tsai, H.-C. Feng, *Eur. Polym. J.* **2009**, *45*, 2348–2357; b) S. Vijayakumar, P. Rajakumar, *ILCPA* **2013**, *4*, 58–65; c) J.-c. Wang, H. Wang, *Sep. Purif. Technol.* **2017**, *187*, 415–425.
- [11] a) Y. Shao, Q. Xia, L. Dong, X. Liu, X. Han, S. F. Parker, Y. Cheng, L. L. Daemen, A. J. Ramirez-Cuesta, S. Yang, Y. Wang, *Nat. Commun.* **2017**, *8*, 16104; b) Q. Xia, Z. Chen, Y. Shao, X. Gong, H. Wang, X. Liu, S. F. Parker, X. Han, S. Yang, Y. Wang, *Nat. Commun.* **2016**, *7*, 11162; c) Q. N. Xia, Q. Cuan, X. H. Liu, X. Q. Gong, G. Z. Lu, Y. Q. Wang, *Angew. Chem. Int. Ed.* **2014**, *53*, 9755–9760; *Angew. Chem.* **2014**, *126*, 9913–9918.
- [12] L. Dong, L. F. Lin, X. Han, X. Q. Si, X. H. Liu, Y. Guo, F. Lu, S. Rudic, S. F. Parker, S. H. Yang, Y. Q. Wang, *Chem* **2019**, *5*, 1521–1536.
- [13] J. Nilsson, P.-A. Carlsson, H. Grönbeck, M. Skoglundh, *Top. Catal.* **2017**, *60*, 283–288.
- [14] a) U. Sanyal, Y. Song, N. Singh, J. L. Fulton, J. Herranz, A. Jentys, O. Y. Gutiérrez, J. A. Lercher, *ChemCatChem* **2019**, *11*, 575–582; b) N. Singh, U. Sanyal, G. Ruehl, K. A. Stoerzinger, O. Y. Gutiérrez, D. M. Camaioni, J. L. Fulton, J. A. Lercher, C. T. Campbell, *J. Catal.* **2020**, *382*, 372–384.
- [15] Y. Jing, Y. Xin, Y. Guo, X. Liu, Y. Wang, *Chin. J. Catal.* **2019**, *40*, 1168–1177.
- [16] a) D. Zhang, A. Duan, Z. Zhao, C. Xu, *J. Catal.* **2010**, *274*, 273–286; b) P. Michaud, J. Lemberton, G. Pérot, *Appl. Catal. A* **1998**, *169*, 343–353.
- [17] M. Segall, P. J. Lindan, M. a. Probert, C. J. Pickard, P. J. Hasnip, S. Clark, M. Payne, *J. Phys. Condens. Matter* **2002**, *14*, 2717.
- [18] B. Hammer, L. B. Hansen, J. K. Nørskov, *Phys. Rev. B* **1999**, *59*, 7413.
- [19] D. Vanderbilt, *Phys. Rev. B* **1990**, *41*, 7892.
- [20] H. Monkshott, J. Pack, *Phys. Rev. B* **1976**, *13*, 5188–5192.
- [21] Y. Yang, P. Bai, X. Guo, *Ind. Eng. Chem. Res.* **2017**, *56*, 14725–14753.

Manuscript received: August 12, 2020

Revised manuscript received: November 23, 2020

Accepted manuscript online: December 2, 2020

Version of record online: January 18, 2021